

From 6 & 12 to 22 GeV

Experimental prospects in Hall B for nucleon's pressure studies



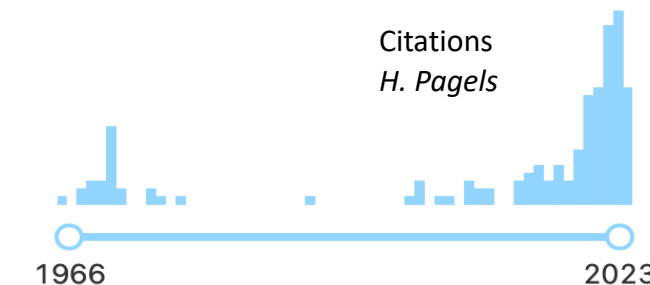
Volker D. Burkert
Jefferson Laboratory

Towards Improved Hadron Femtography with Hard Exclusive Reactions
Jefferson Lab, August 7-11, 2023

Mechanical properties of particles

- What are mechanical properties of nucleons?
 - The internal distribution of forces and pressure
 - The distribution of mass and energy
 - The distribution of angular momentum
 - The physical size as given by the mechanical radius
- These fundamental properties, in principle, can be probed directly in the short distance interaction of nucleons with gravitons, which is experimentally not realizable.
- Although the theoretical framework had been developed in the 1960's, there was not a known way to experimentally access any of these properties in other ways.

*Yu. Kobzarev and L.B. Okun, JETP 16, 5 (1963);
H. Pagels, Phys. Rev. 144 (1966) 1250-1260;*

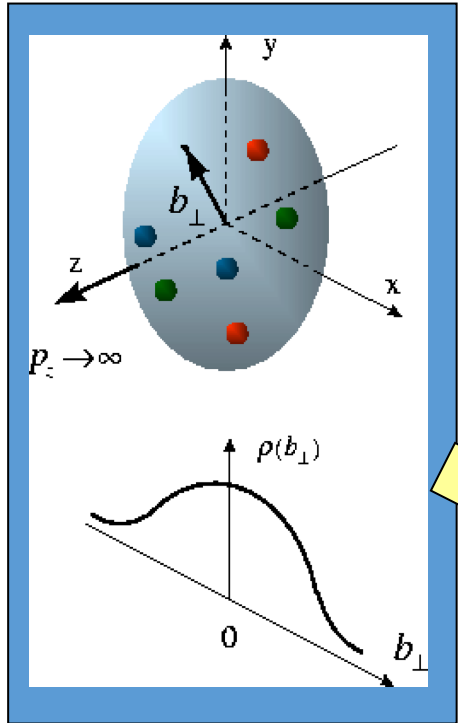


- The development of the generalized parton distributions framework in the mid 1990's, and the discovery of Deeply Virtual Compton Scattering (DVCS) as a means of accessing them, opened the new direction of hadron 3D-imaging.
- It also led to the insight that GPDs can be related to the mechanical properties of nucleons (M. Polyakov, 2003).

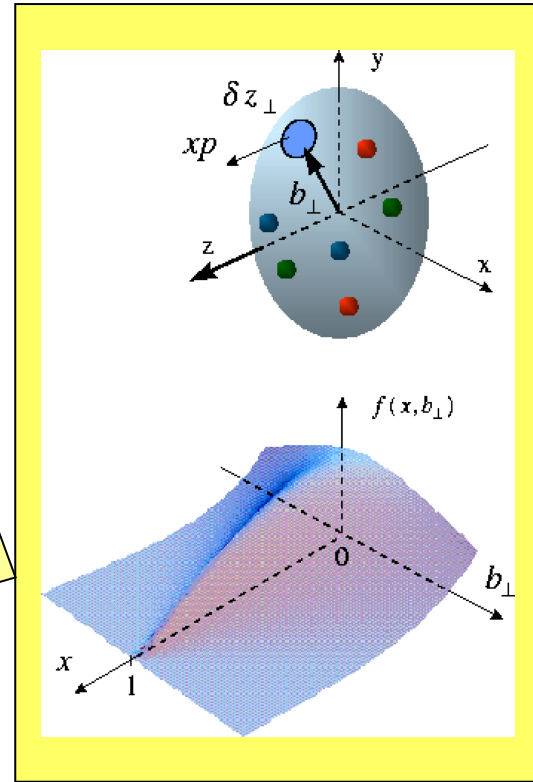
GPDs and 3D Imaging of Nucleons

X. Ji, D. Mueller, A. Radyushkin; 1994-1997

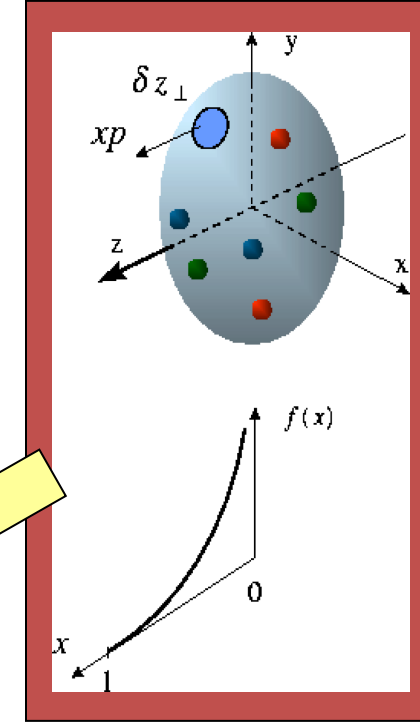
A.V. Belitsky



Elastic form factors →
Transverse charge & current
densities $F_1(t)$, $F_2(t)$.

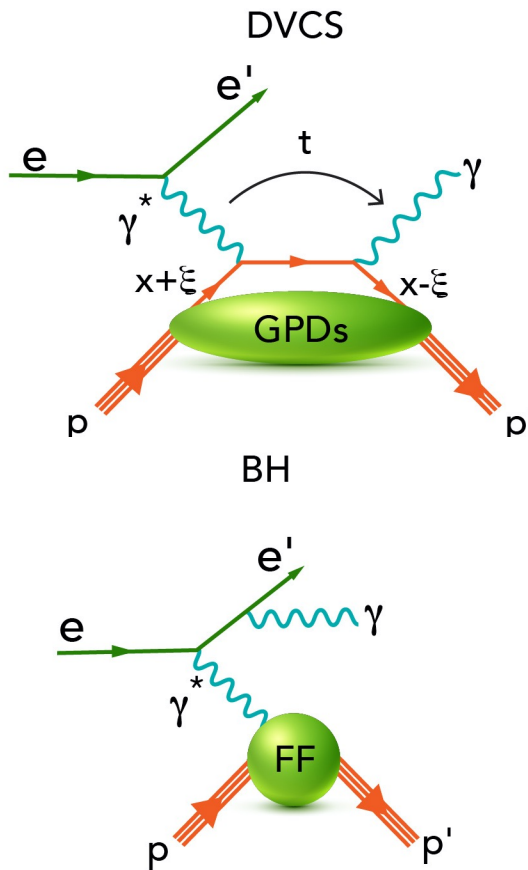


Deeply exclusive processes → GPD's
and (2+1)D images in transverse space
and longitudinal momentum.
4 chiral even GPDs $H, E, \tilde{H}, \tilde{E}(x, \xi, t)$



DIS structure functions
→ Longitudinal parton
momentum & helicity
densities, $F_2(x)$, $g_1(x)$.

DVCS → probing GPDs → 3D imaging



$$\xi \sim x_B / (2 - x_B)$$

$$k = t / 4M^2$$

Polarized beam, unpolarized target:

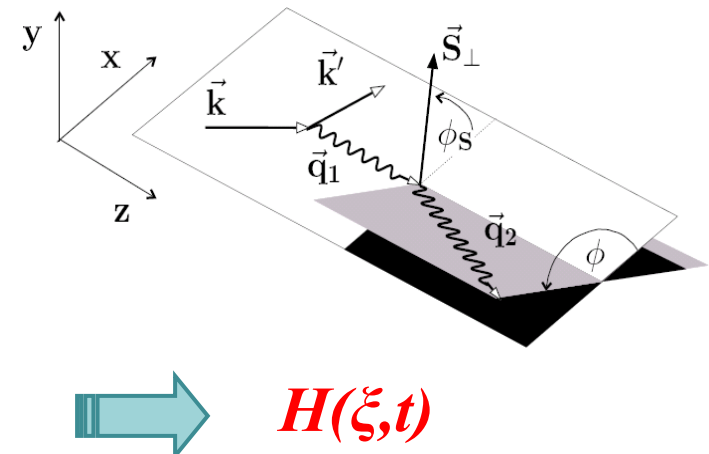
$$\Delta\sigma_{LU} \sim \sin\phi \operatorname{Im}\{F_1 \mathbf{H} + \xi(F_1 + F_2) \tilde{\mathbf{H}} + kF_2 \mathbf{E}\} d\phi$$

Unpolarized beam, longitudinal target:

$$\Delta\sigma_{UL} \sim \sin\phi \operatorname{Im}\{F_1 \tilde{\mathbf{H}} + \xi(F_1 + F_2)(\mathbf{H} + \xi/(1+\xi) \mathbf{E})\} d\phi$$

Unpolarized beam, transverse target:

$$\Delta\sigma_{UT} \sim \cos\phi \sin(\phi_s - \phi) \operatorname{Im}\{k(F_2 \mathbf{H} - F_1 \mathbf{E})\} d\phi$$



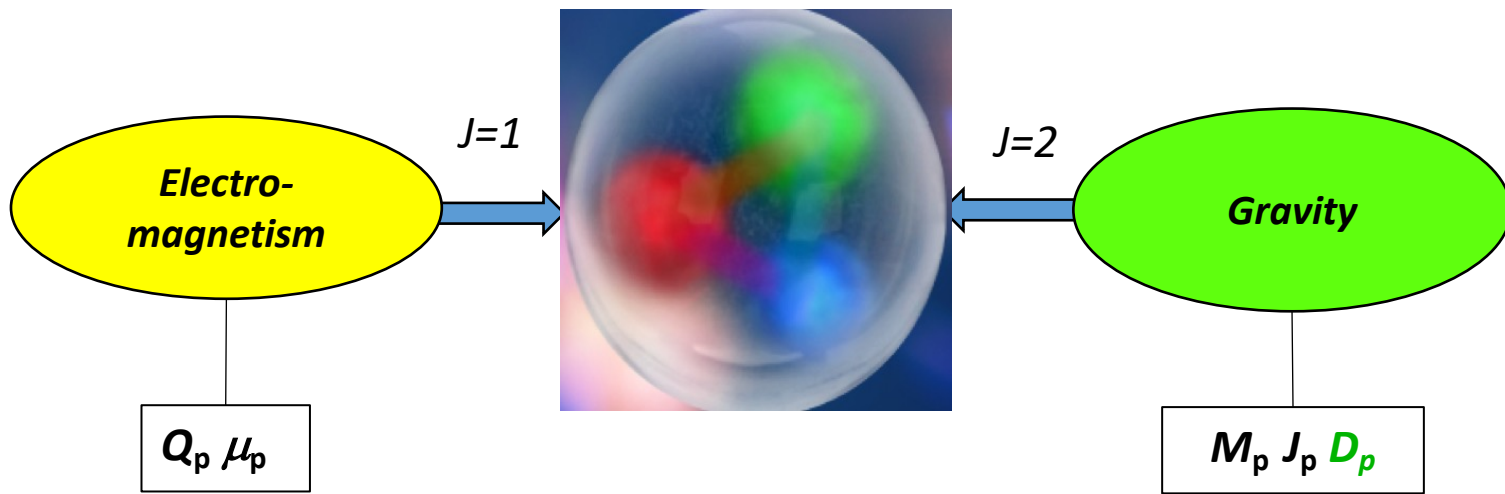
$$\mathbf{H}(\xi, t)$$

$$\tilde{\mathbf{H}}(\xi, t)$$

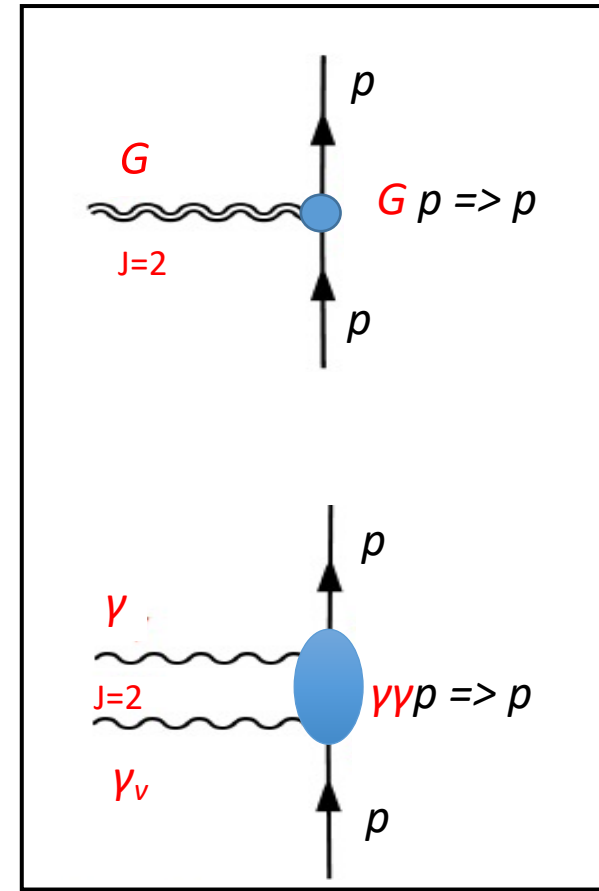
$$\mathbf{E}(\xi, t)$$

A.V. Belitsky, D. Mueller, A. Kirchner, Nucl.Phys. B629 (2002) 323-3922002

Probing structural properties of the proton



- DVCS as substitute that mimics graviton-proton interaction.



*Misner, C.W.; K. S. Thorne; J. A. Wheeler (1973).
Gravitation, W.H. Freeman, ISBN 0-7167-0344-0.*

The 2γ field couples to the EMT as gravity does with many orders of magnitude greater strength.

EMT & Gravitational Form Factors (GFF)

Gravitational form factor of the EMTs

$$\begin{aligned} \langle p', \vec{s}' | T_a^{\mu\nu}(0) | p, \vec{s} \rangle &= \bar{u}(p', \vec{s}') \left[A_a(t) \frac{P^\mu P^\nu}{M_N} \right. \\ &+ \boxed{D_a(t)} \frac{\Delta^\mu \Delta^\nu - g^{\mu\nu} \Delta^2}{4M_N} + \bar{C}_a(t) M_N g^{\mu\nu} \quad \text{c.c.} \\ &\left. + \boxed{J_a(t)} \frac{P^{\{\mu} i\sigma^{\nu\}}\lambda \Delta_\lambda}{M_N} - S_a(t) \frac{P^{[\mu} i\sigma^{\nu]\lambda} \Delta_\lambda}{M_N} \right] u(p, \vec{s}) \\ &\qquad a = q, G \end{aligned}$$

2nd Mellin Moments of GPDs

$$\int_{-1}^1 dx x H_q(x, \xi, t) = \boxed{A_q(t)} + \xi^2 \boxed{D_q(t)}$$

$$\int_{-1}^1 dx x E_q(x, \xi, t) = B_q(t) - \xi^2 \boxed{D_q(t)}$$

$$B_q(t) = 2 \boxed{J_q(t)} - A_q(t)$$

GPDs → Compton Form Factors (CFFs)

$$\begin{aligned} \text{Re}\mathcal{H}(\xi, t) + i \text{Im}\mathcal{H}(\xi, t) &= \\ \sum_q e_q^2 \int_{-1}^1 dx \left[\frac{1}{\xi - x - i\epsilon} - \frac{1}{\xi + x - i\epsilon} \right] H_q(x, \xi, t) \end{aligned}$$

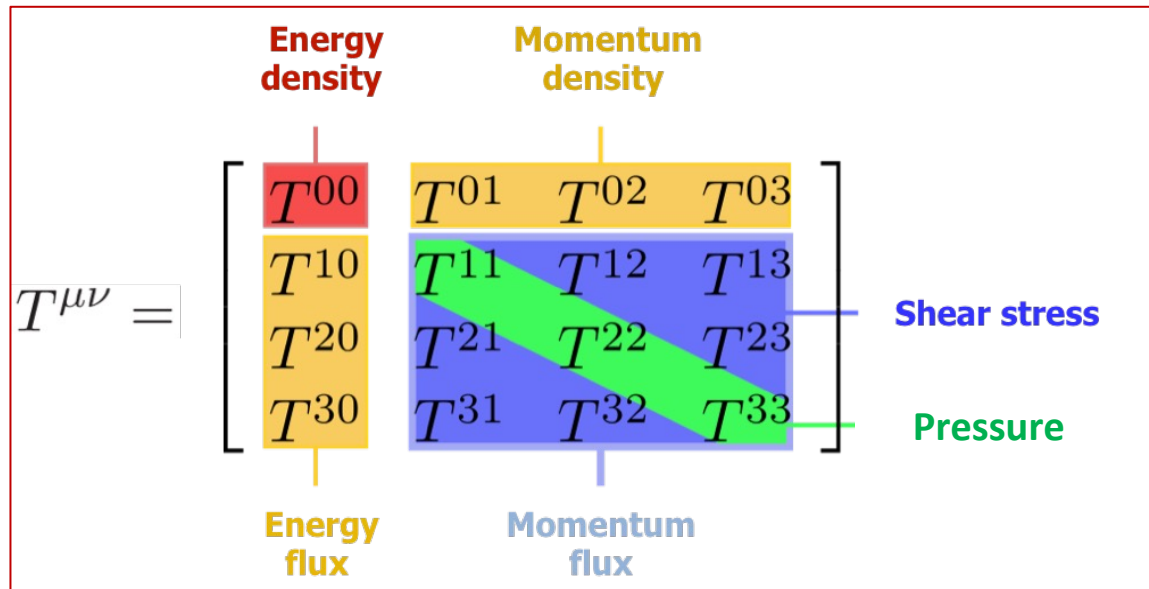
Fixed-t subtracted dispersion relation

$$\begin{aligned} \text{Re}\mathcal{H}(\xi, t) &= \boxed{\mathcal{C}_{\mathcal{H}}(t)} \\ &+ \frac{1}{\pi} \text{P.V.} \int_0^1 d\xi' \left[\frac{1}{\xi - \xi'} - \frac{1}{\xi + \xi'} \right] \text{Im}\mathcal{H}(\xi', t) \end{aligned}$$

$$\boxed{\mathcal{C}_{\mathcal{H}}(t)} = 2 \sum_q e_q^2 \int_{-1}^1 dz \frac{D_{\text{term}}^q(z, t)}{1 - z} \quad z = \xi/x$$

$$D_{\text{term}}^q(z, t) = (1 - z^2) \sum_{\text{odd } n} \boxed{d_n^q(t)} C_n^{3/2}(z) \quad \longrightarrow \quad n=1$$

Energy Momentum Tensor $T^{\mu\nu}$



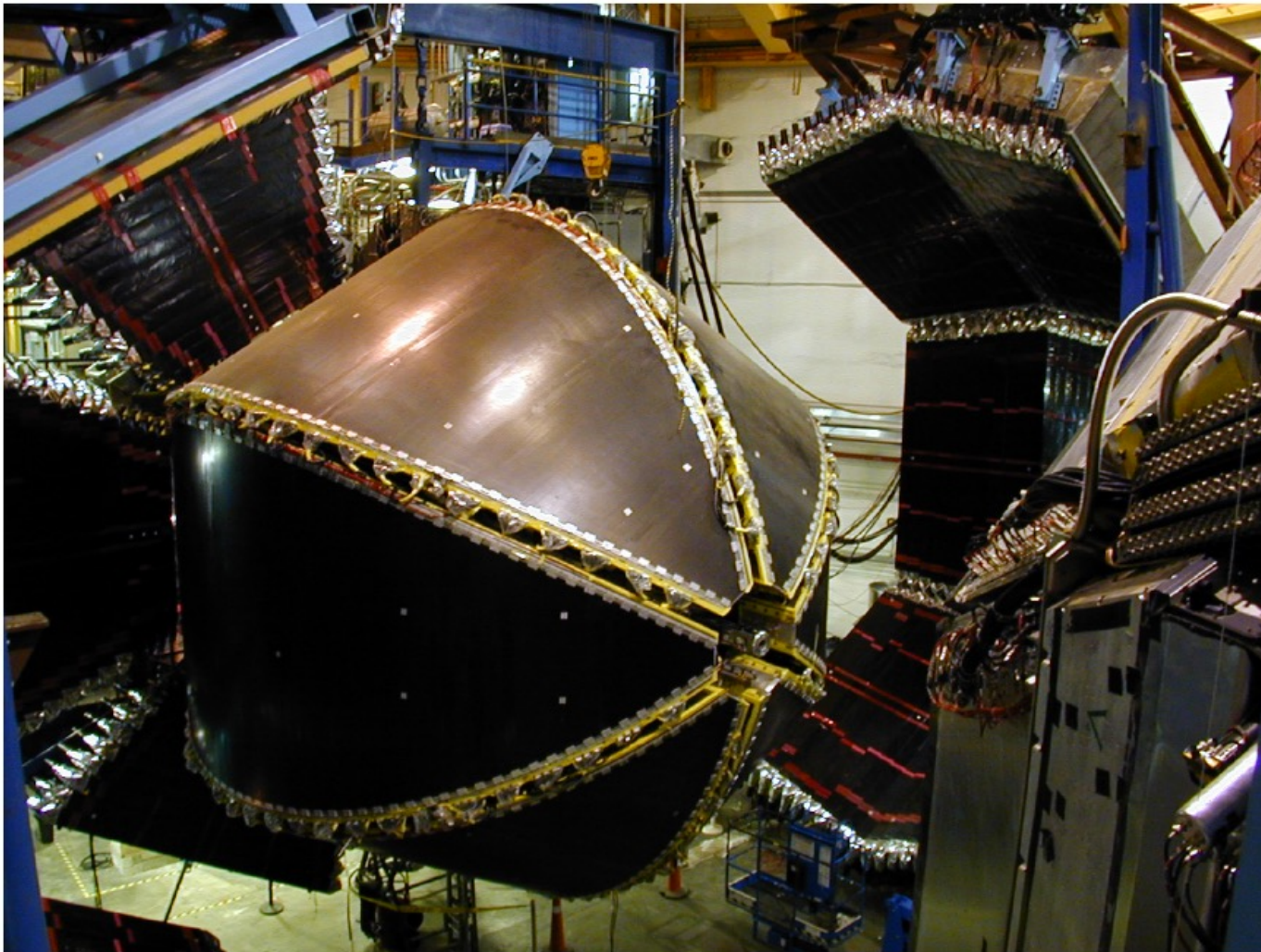
$$T^{ij}(\mathbf{r}) = \left(\frac{r^i r^j}{r^2} - \frac{1}{3} \delta^{ij} \right) s^Q(r) + \delta^{ij} p^Q(r)$$

$$d_1^Q(t) = 5M_p \int d^3\mathbf{r} \frac{j_2(r\sqrt{-t})}{t} s^Q(r)$$

$$d_1^Q(t) = 15M_p \int d^3\mathbf{r} \frac{j_0(r\sqrt{-t})}{2t} p^Q(r)$$

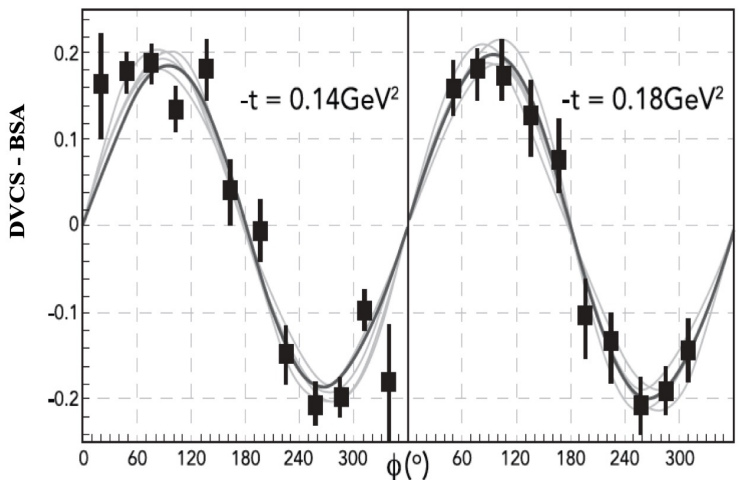
j_0, j_2 Spherical Bessel functions

CLAS @ 6 GeV

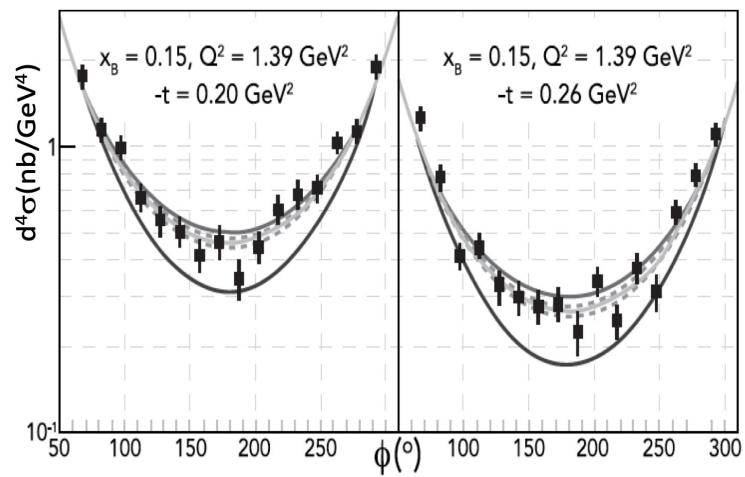


In operation until 2012

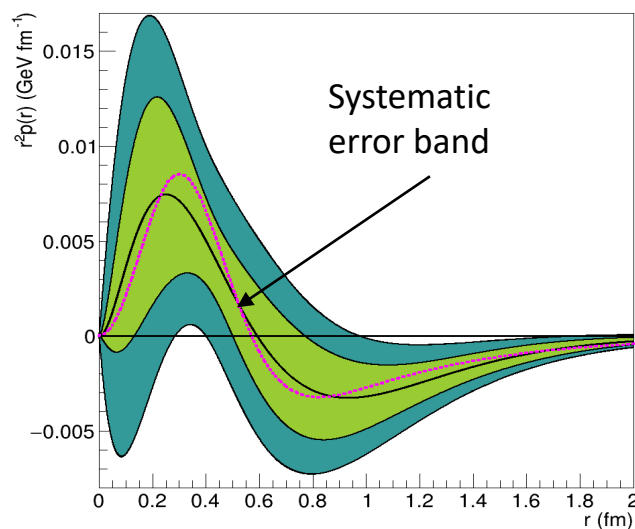
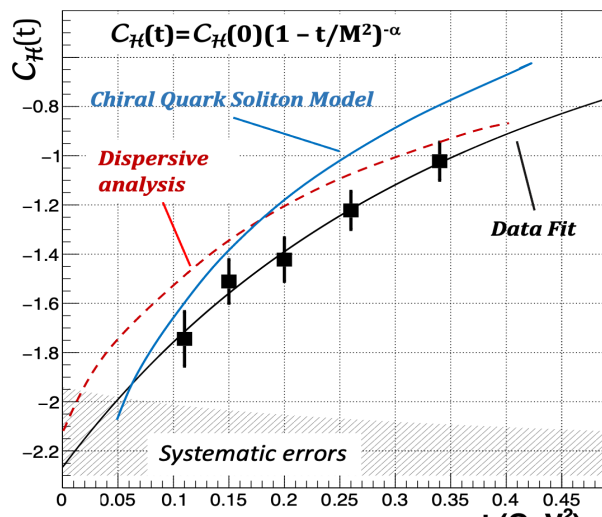
DVCS with CLAS @ 6 GeV



F.X. Girod et al., Phys.Rev.Lett. 100 (2008) 162002

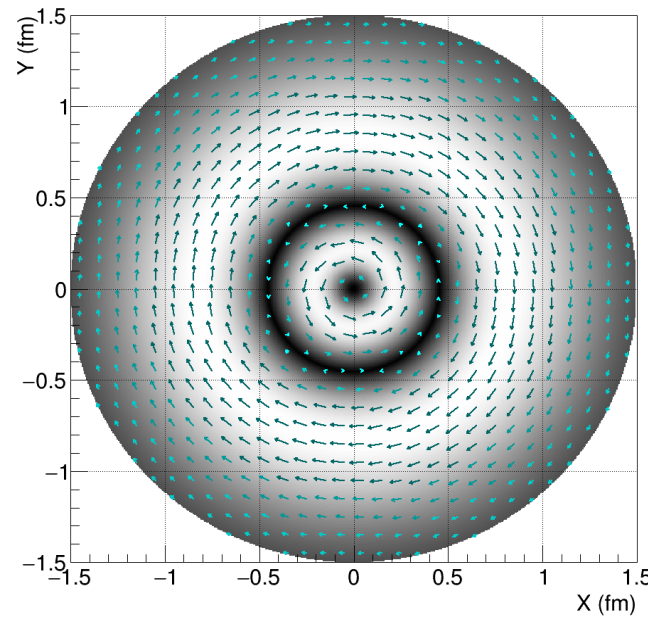


H.S. Jo et al., Phys.Rev.Lett. 115 (2015) 21, 212003

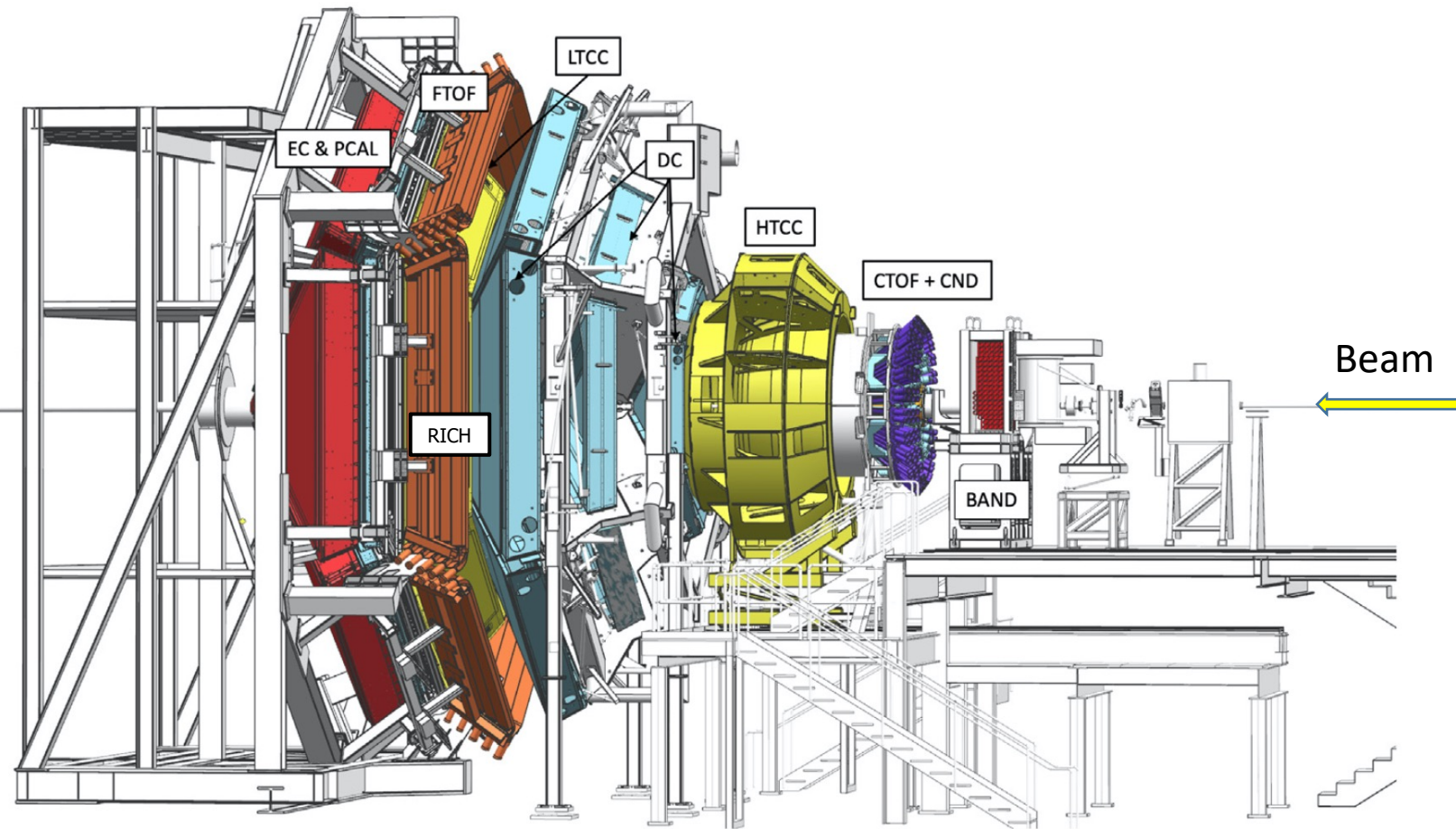


V.B., L. Elouadrhiri, F.X. Girod, C. Lorce, P. Schweitzer, P. Shanahan; to appear in: Review of Modern Physics, 2023

Tangential stress in Proton



The CLAS12 Spectrometer at Jefferson Lab



Baseline equipment

Forward Detector (FD)

- TORUS magnet (6 coils)
- HT Cherenkov Counter
- Drift Chamber System
- LT Cherenkov Counter
- Forward ToF System
- Pre-Shower Calorimeter
- E.M. Calorimeter
- RICH (2 sectors)

Central Detector (CD)

- SOLENOID magnet (5T)
- Central Tracker (SVT, MM)
- Central Time-of-Flight
- Central Neutron Detector

Beamline

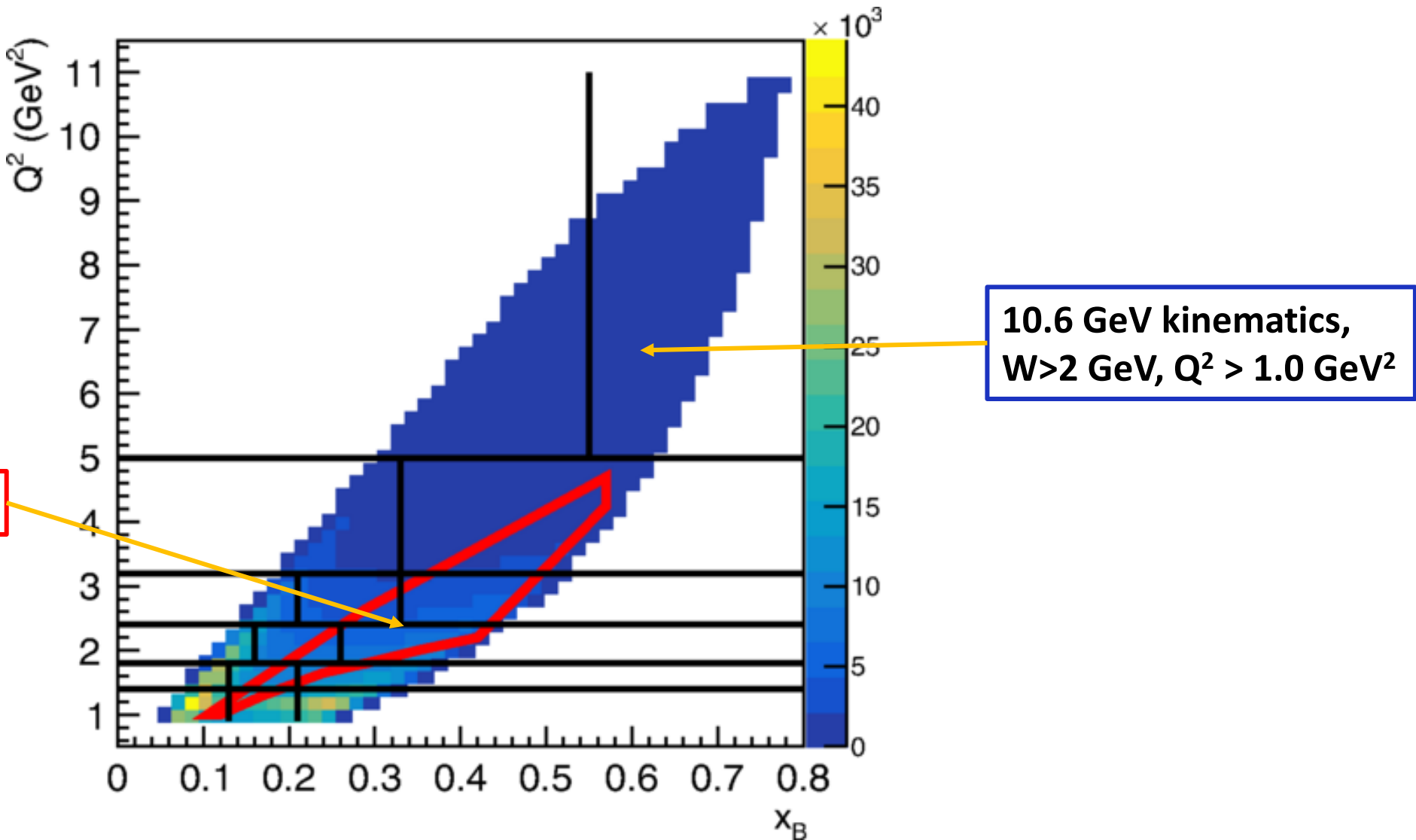
- Liquid & solid targets
- Moller Polarimeter

Ancillary equipment

- Forward Tagger
- Long. Polarized Target
- Trans. Polarized Target (planned)

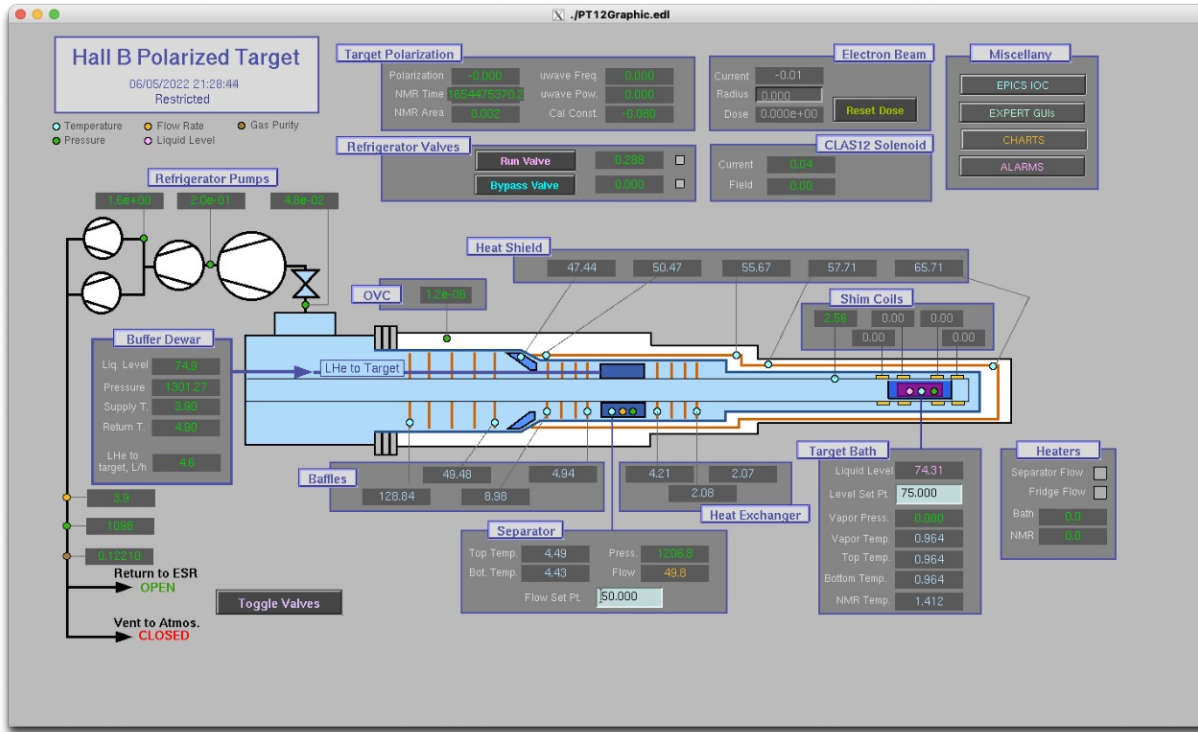
Nuclear Inst. and Methods in Physics Research, A 959 (2020) 163419 + 17 articles on all subsystems.

CLAS12 DIS coverage in Q^2 , x_B @ 10.6 GeV



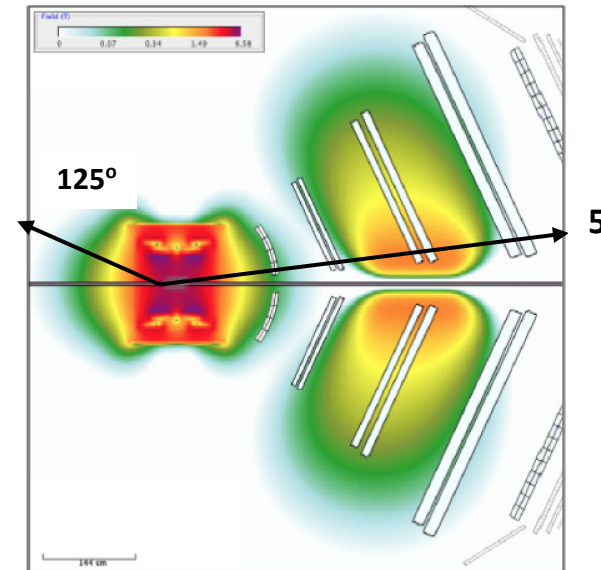
Longitudinally polarized target for CLAS12

In use to measure DVCS and other processes on polarized protons and deuterons (neutrons).



Courtesy C. Keith

CLAS12 5T solenoid magnet used as the polarizing field for the dynamically polarized ammonia target.



Longitudinal polarized target
Operational with full CLAS12 acceptance.

$$\Delta\sigma_{UL} \sim \sin\phi \operatorname{Im}\{F_1 \tilde{H} + \xi(F_1 + F_2)(\mathbf{H} + \xi/(1+\xi)\mathbf{E})\} d\phi$$

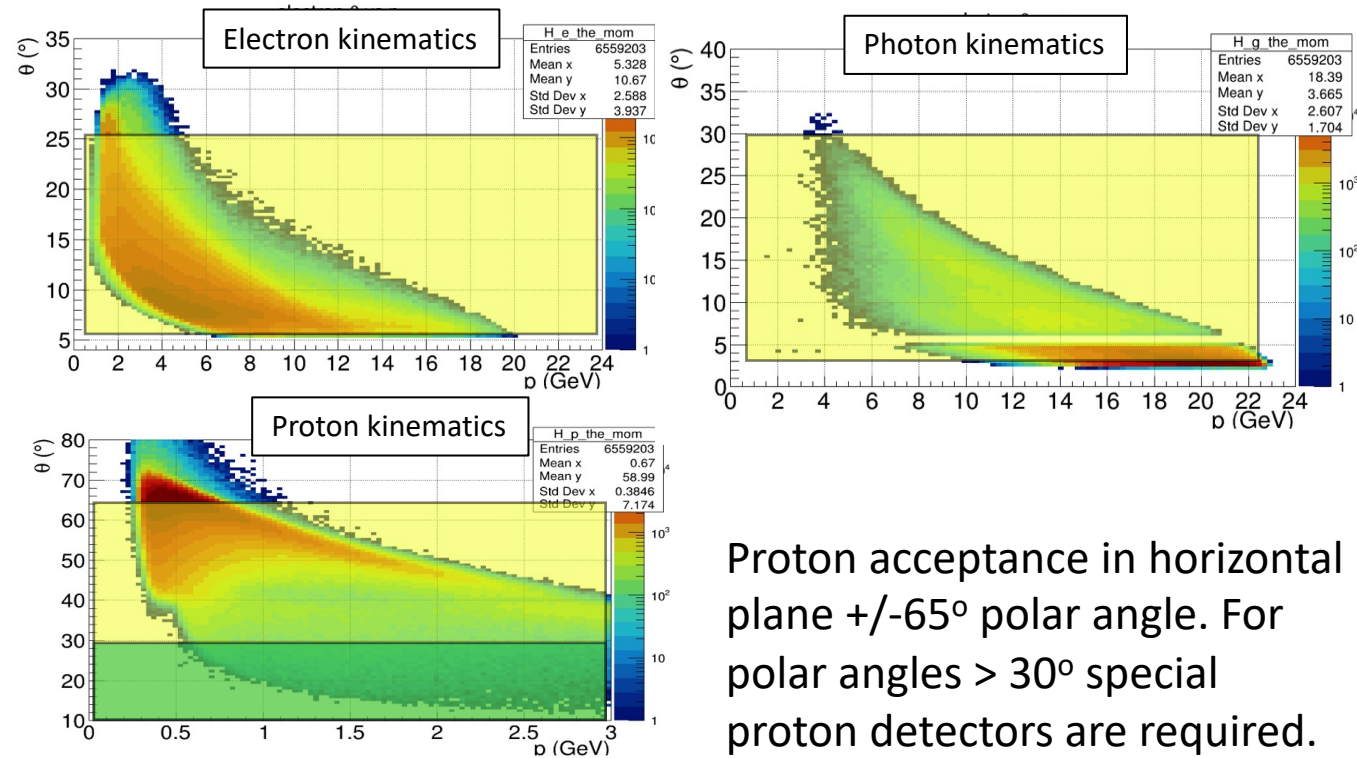
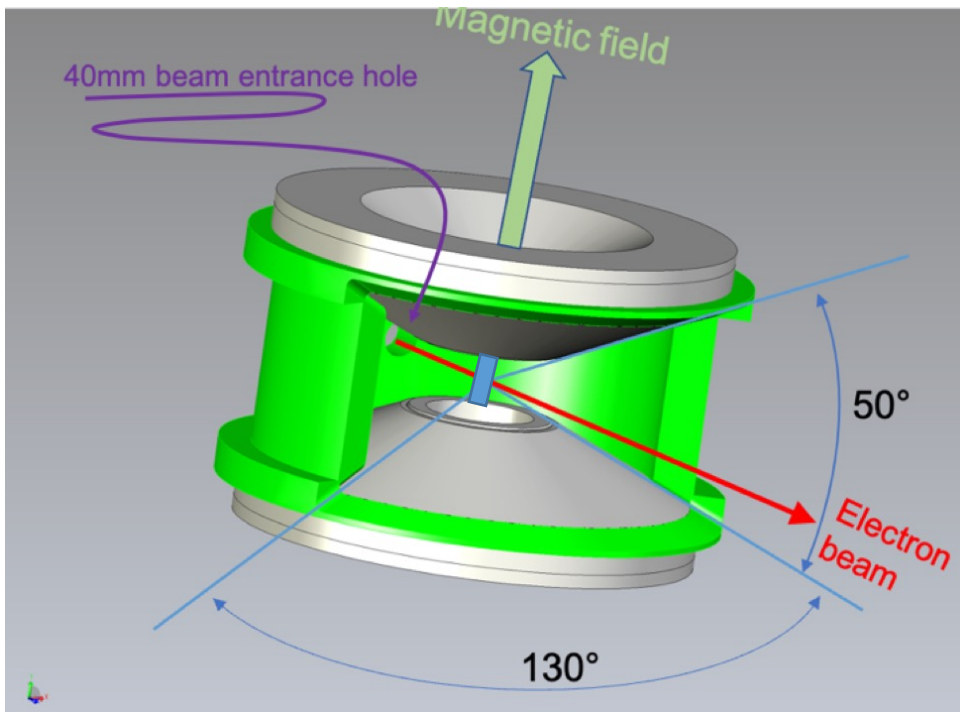
→ RG-C run group completed this spring, analysis in progress.

DVCS @ Transverse polarized target

Unpolarized beam, **transverse** target:

$$\Delta\sigma_{UT} \sim \cos\phi \sin(\phi_s - \phi) \text{Im}\{k(F_2 \mathbf{H} - F_1 \mathbf{E})\} d\phi$$

→ RG-H run group 110 PAC days
(incl. 3 A rated experiments)



Proton acceptance in horizontal plane +/-65° polar angle. For polar angles > 30° special proton detectors are required.

- **Transverse polarized target in development for RG-H experiments.**

P. Ghoshal
C. Keith

DVCS@10.6 GeV – RGA, RGB, RGC, RGH



Status and prospects of DVCS at 11 GeV

RGA

Unpolarized protons in IH_2 target

Beam spin asymmetry:

G. Christiaens, PRL 130 (2023) 21, 211902

Diff. cross sections

S. Lee, *in preparation*

Sensitivity to CFF \mathcal{H}_p

RGB

Unpolarized protons & neutrons in ID_2

n(p) BSA: A. Hobart, *in prep.*

p(n) BSA: A. Hobart, *in prep.*

Sensitivity to CFF $\mathcal{H}_p \mathcal{E}_n$

RGC

Polarized electrons at 10.6 GeV on long. polarized proton NH_3 and polarized deuterium ND_3 .

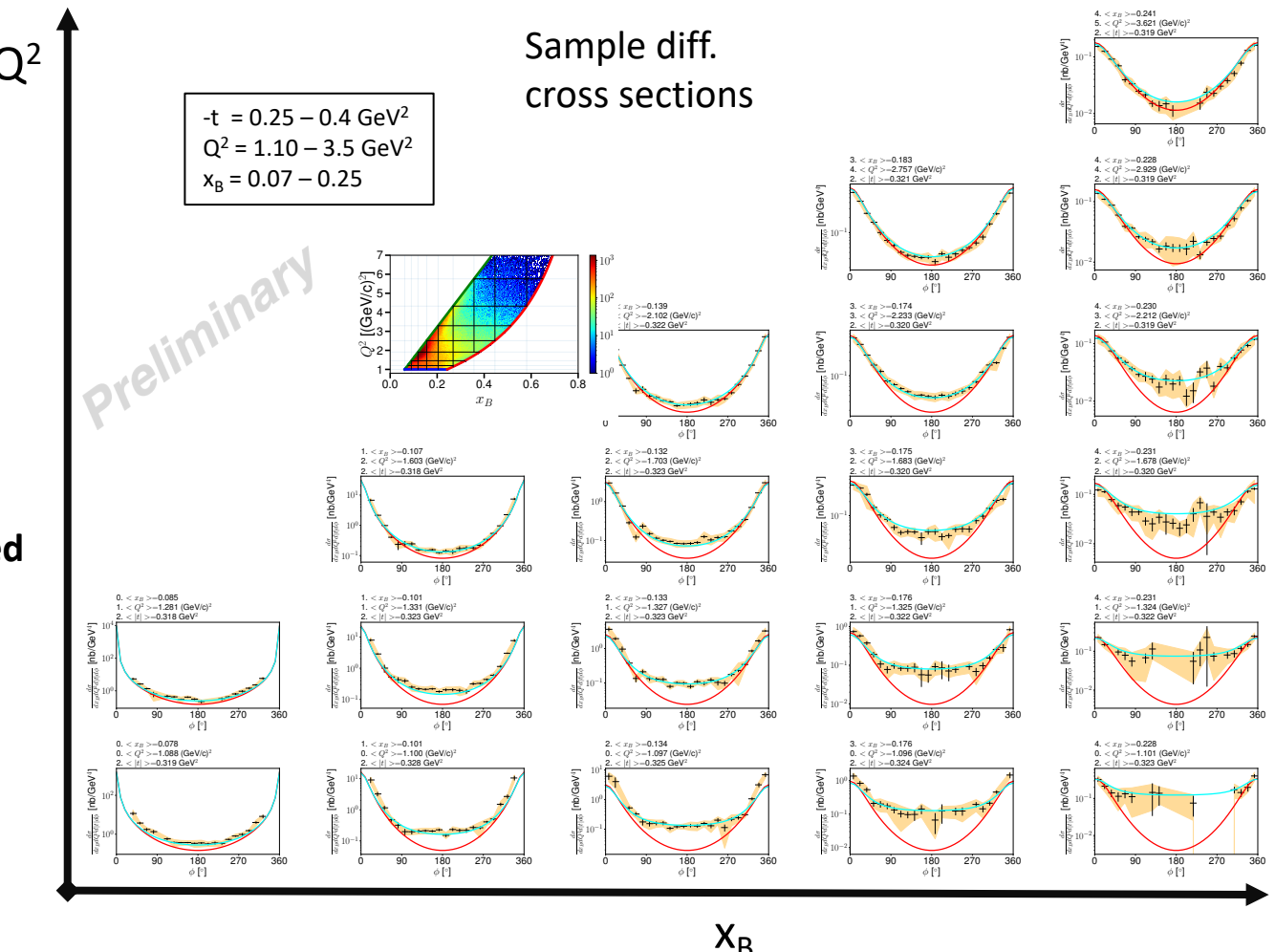
Experiment complete.

Sensitivity to CFF $\tilde{\mathcal{H}}_p$

RGH

Polarized electrons at 10.6 GeV on transverse polarized proton in NH_3 . Target in design stage.

Sensitivity to CFF \mathcal{E}_p

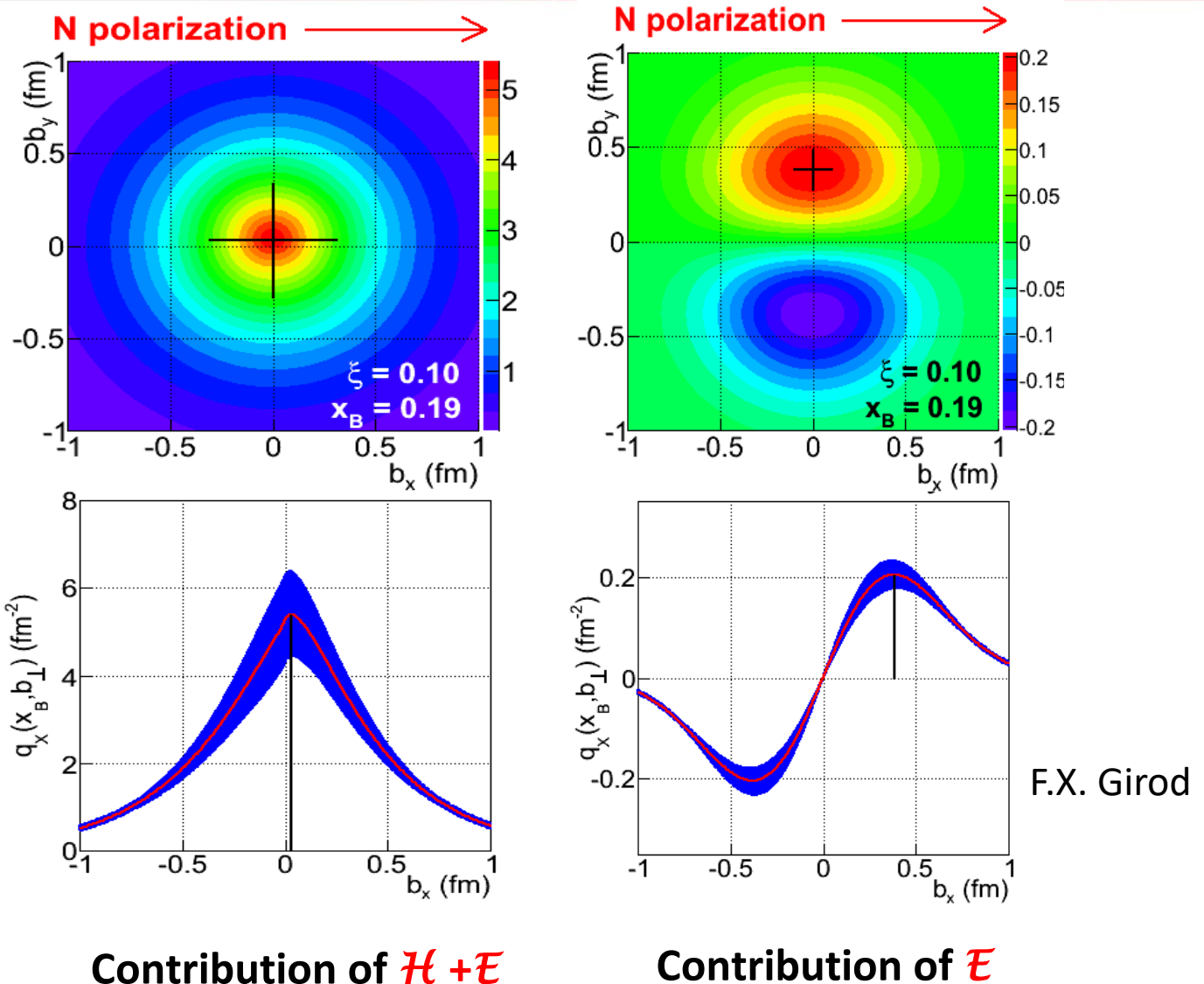


3D imaging of quarks in the proton

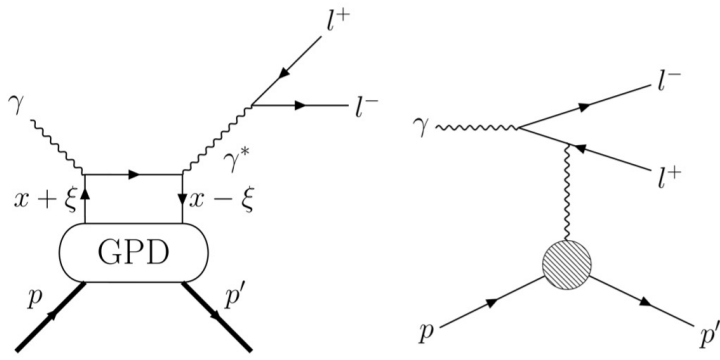
- Model analysis from simulated data (VGG Model) with CLAS12 response.
- From the DVCS cross section and polarization observables the Compton Form Factors $\mathcal{H}(\xi, t)$, $\mathcal{E}(\xi, t)$ may be determined.
- A Fourier transform in t in LC kinematics determines the quark distribution in impact parameter(b_x, b_y) space at fixed $\xi(x_B)$

$$\rho_{\mathcal{H}}(x, \vec{b}_\perp) = \int \frac{d^2 \vec{\Delta}_\perp}{(2\pi)^2} \left[H(x, 0, t) - \frac{E(x, 0, t)}{2M} \frac{\partial}{\partial b_y} \right] e^{-i \vec{\Delta}_\perp \cdot \vec{b}_\perp}$$

M. Burkardt



Time-like Compton Scattering at 10.6 GeV



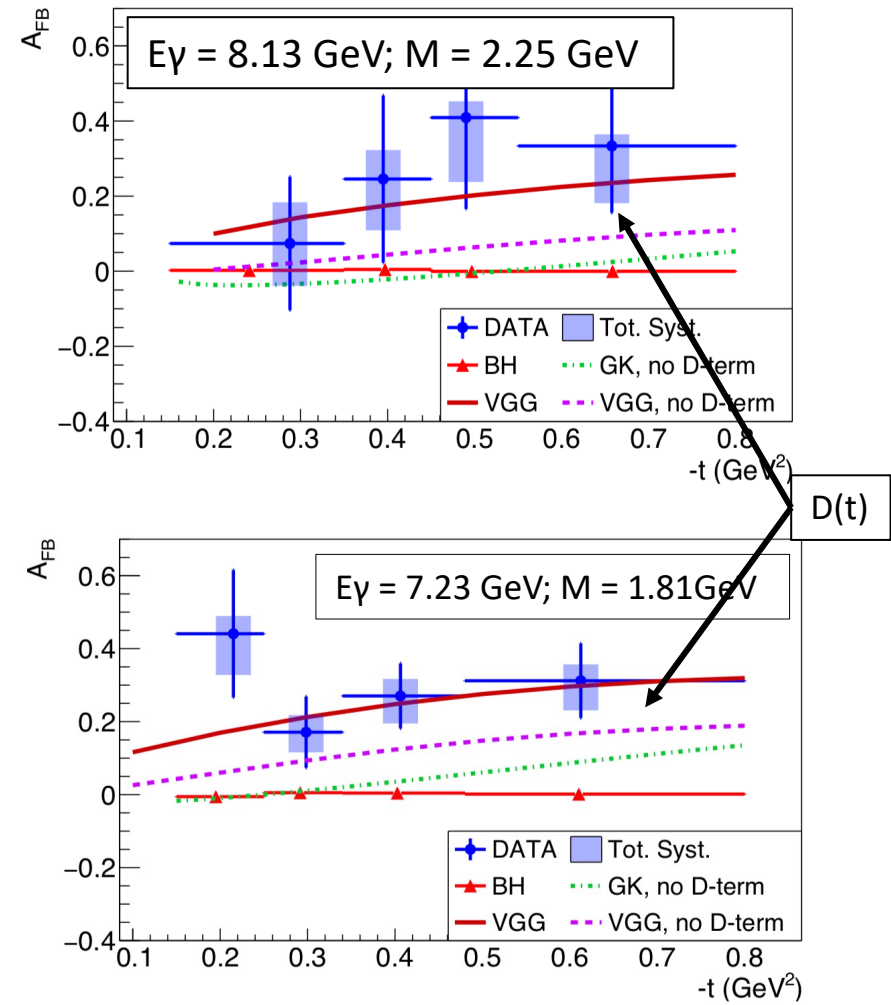
In addition to the BSA from the polarized beam, TCS has a forward-backward asymmetry, which **directly** relates to $\text{Re}\mathcal{H}$ through the interference term with BH.

$$A_{FB}(\theta, \phi) = \frac{d\sigma(\theta, \phi) - d\sigma(180^\circ - \theta, 180^\circ + \phi)}{d\sigma(\theta, \phi) + d\sigma(180^\circ - \theta, 180^\circ + \phi)},$$

$$\frac{d^4\sigma_{INT}}{dQ'^2 dt d\Omega} = A \frac{1 + \cos^2 \theta}{\sin \theta} [\cos \phi \underline{\text{Re} \tilde{M}^{--}} - \nu \cdot \sin \phi \text{Im} \tilde{M}^{--}]$$

$$\tilde{M}^{--} = \left[F_1 \mathcal{H} - \xi(F_1 + F_2) \tilde{\mathcal{H}} - \frac{t}{4m_p^2} F_2 \mathcal{E} \right]$$

→ Effect of $D(t)$ on A_{FB} asymmetry consistent with 6 GeV DVCS results.



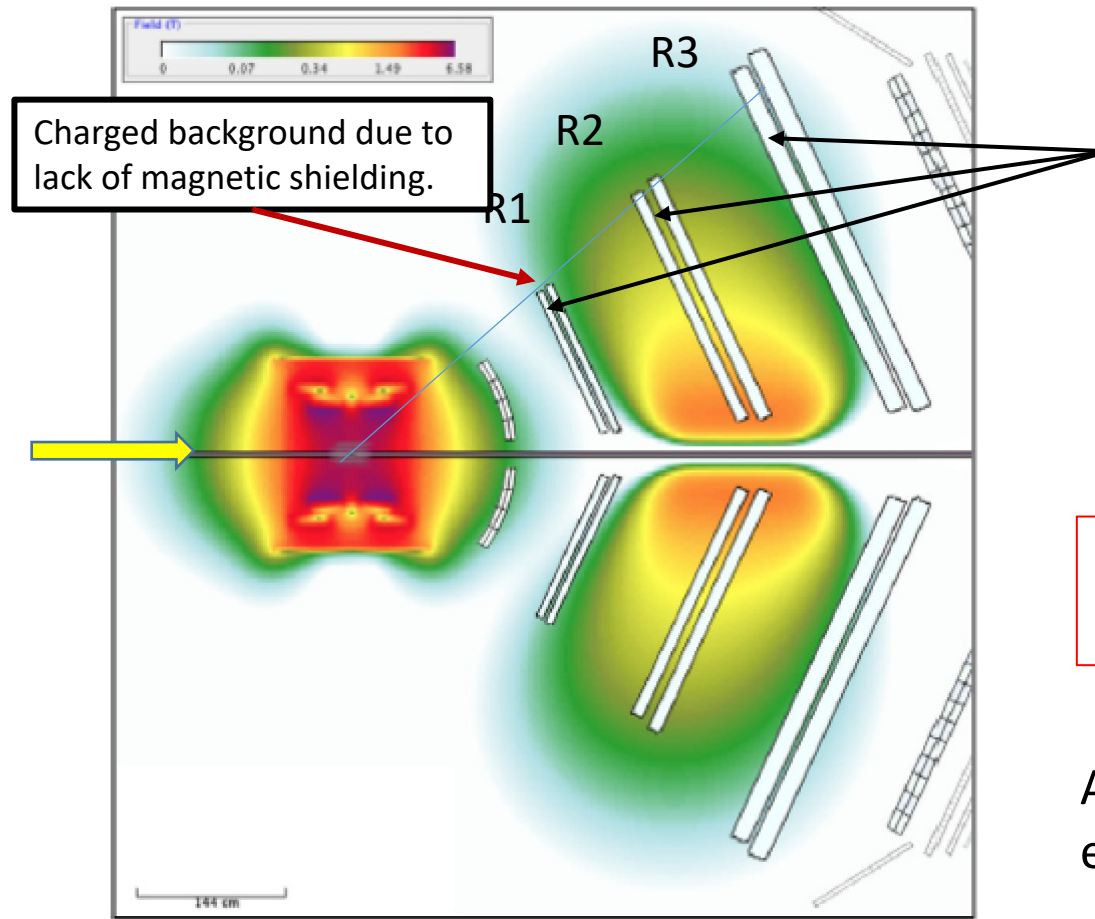
P. Chatagnon et al. PRL.127 (2021) 26, 262501

CLAS12 at 22(24) GeV?

- Can CLAS12 deliver the science of mechanical properties at 22 GeV?
 - Luminosity
 - Acceptance
 - Particle ID
 - Resolution
 - Kinematic reach in $D(t)$

CLAS12 to operate @ 24GeV at 10.6 GeV luminosities?

- CLAS12 luminosity limited by accidental occupancy of DC R1.



High occupancy in part of R1 limits acceptable operating luminosity.
→ higher resolution tracking layers

	R1	R2	R3
CLAS12 @ 11	2.6%	0.76%	1.18%
CLAS12 @ 22	2.8%	0.77%	1.23%

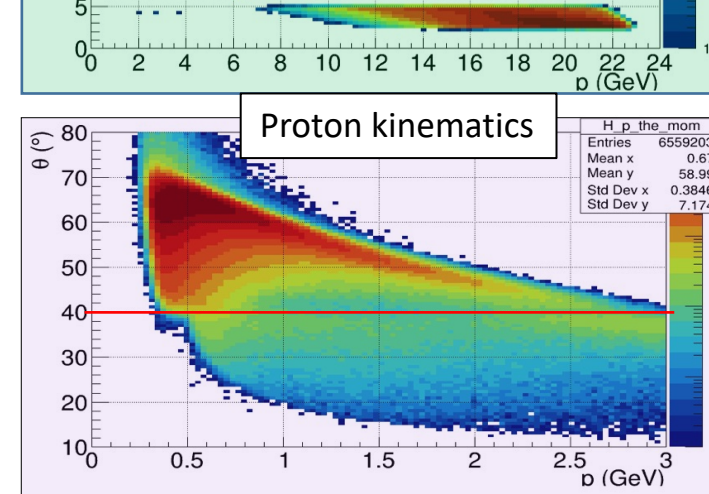
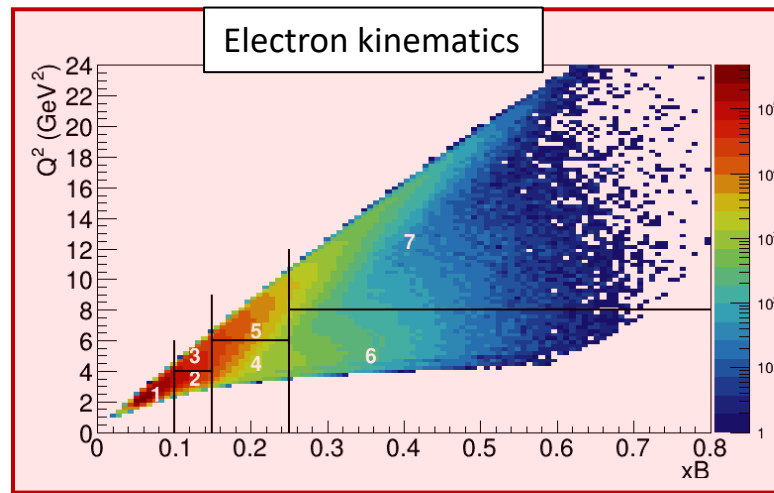
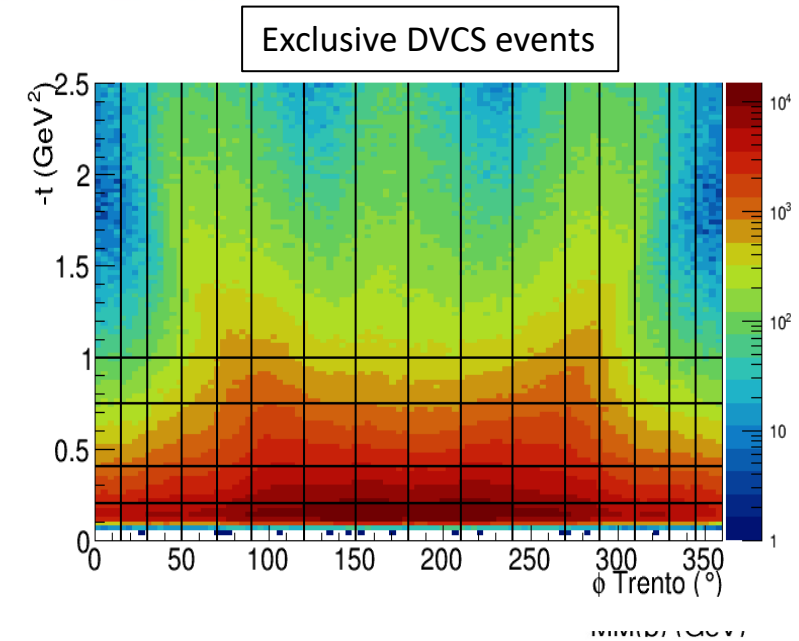
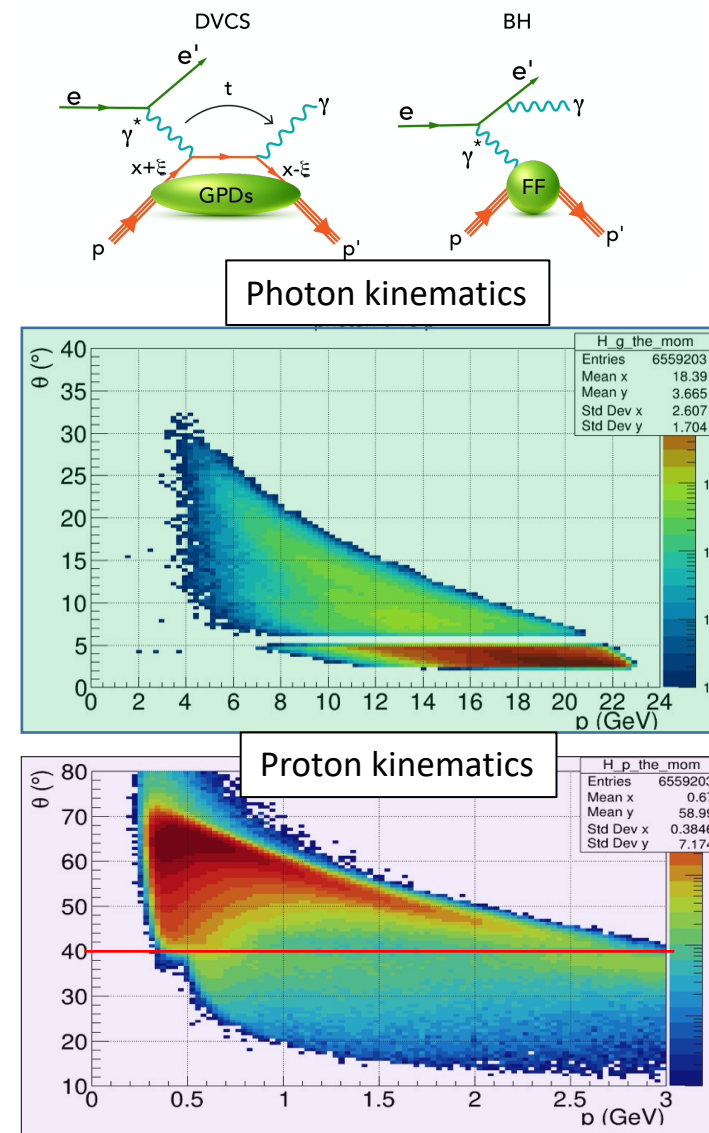
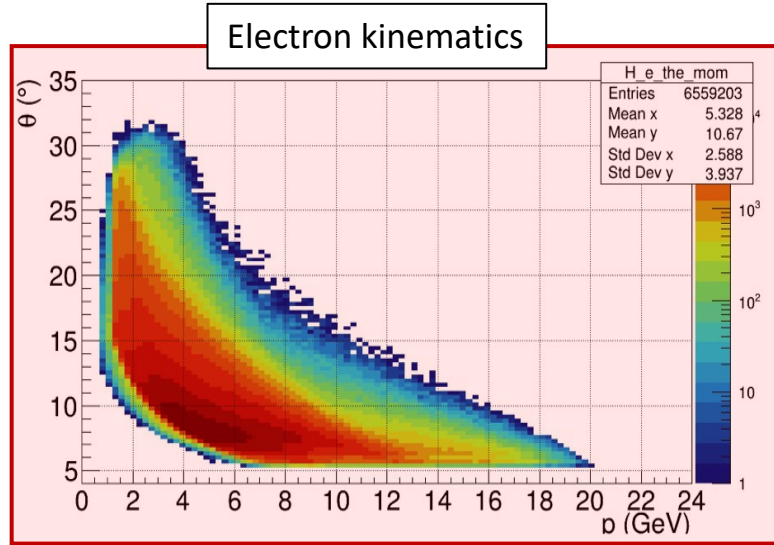
Z. Meador,
L. Elouadrhiri

Accidental occupancies increase by less than 10% at 24 GeV compared to 11 GeV.

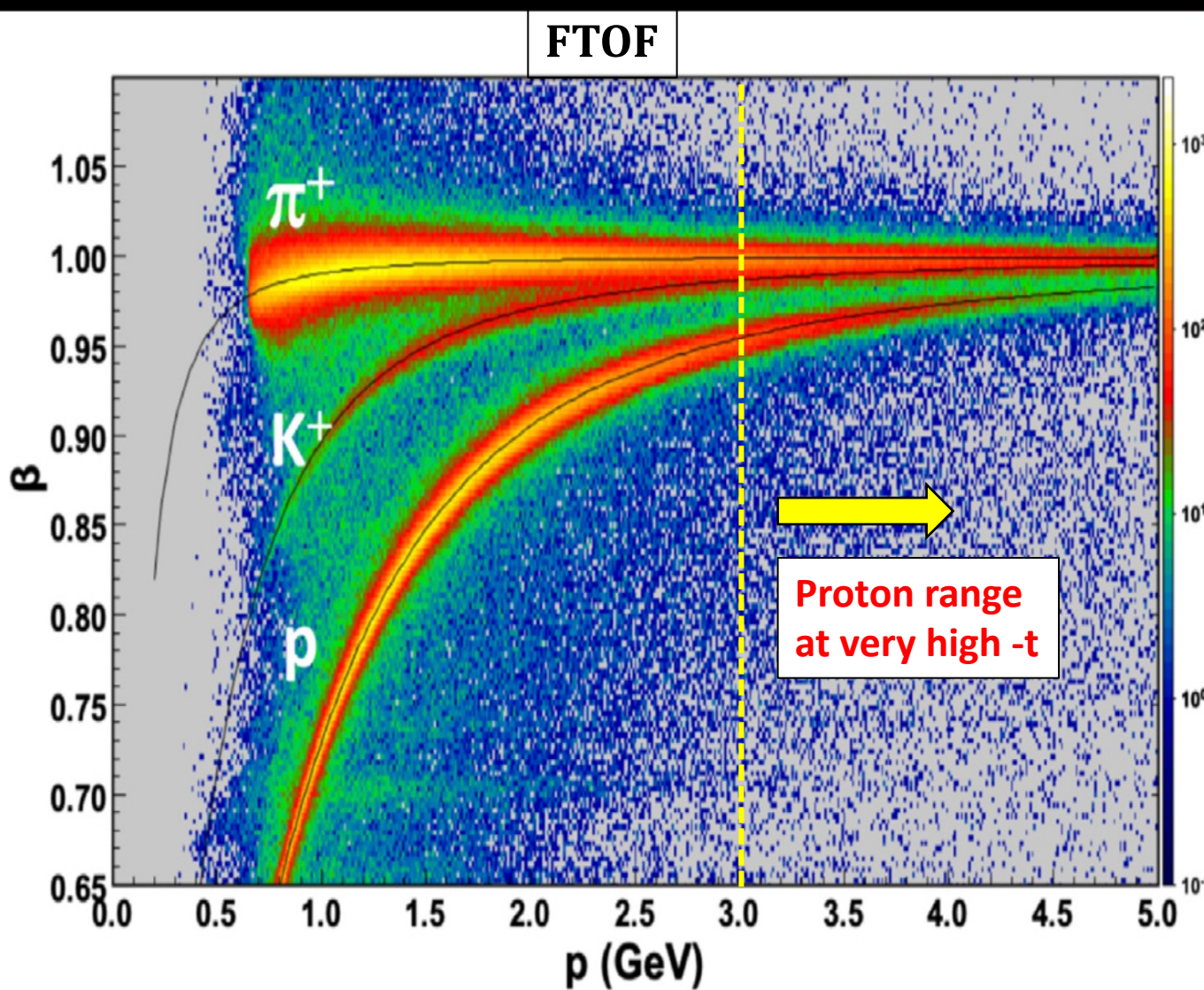
Additional μ -RWELL tracking layers under development enabling increase in CLAS12 operating luminosity by 2.

S. Stepanyan

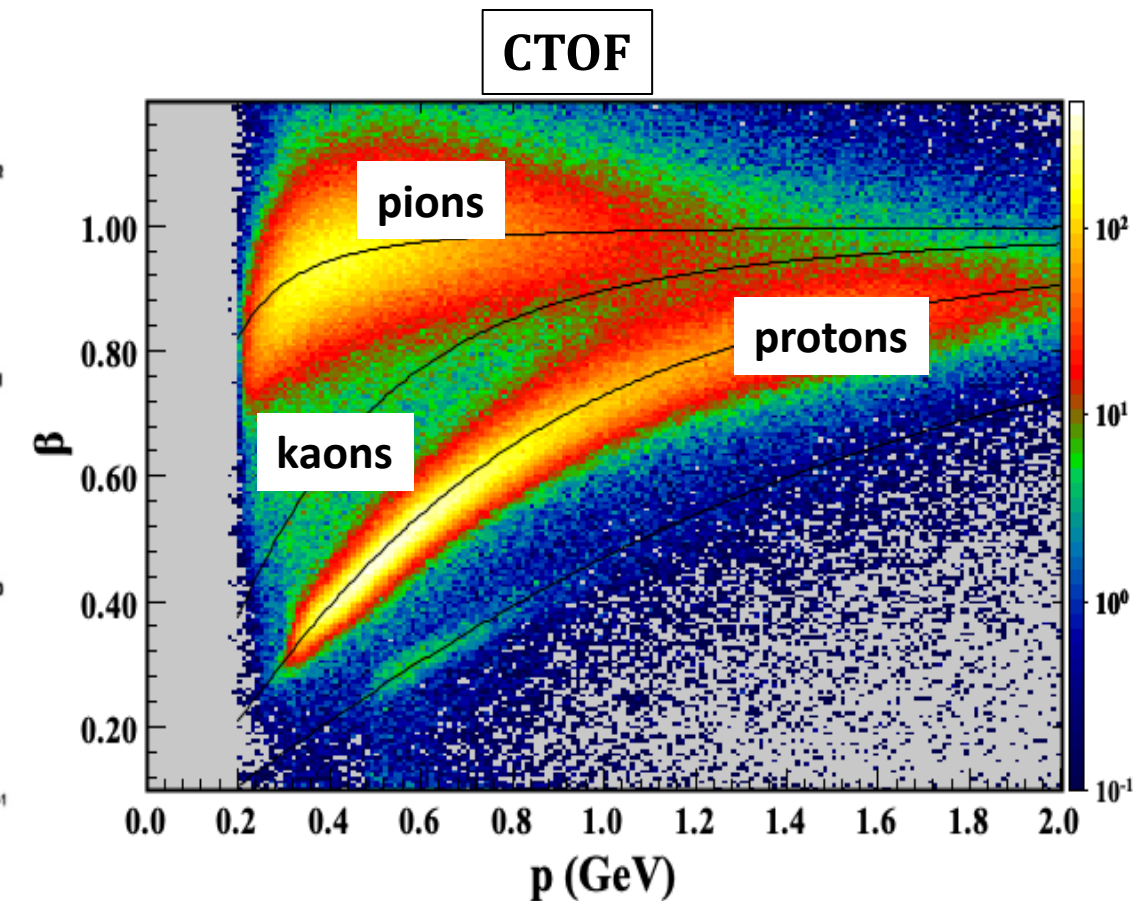
DVCS @ 24 GeV – electron – photon – proton reconstruction



CLAS12 Charged Particle Identification



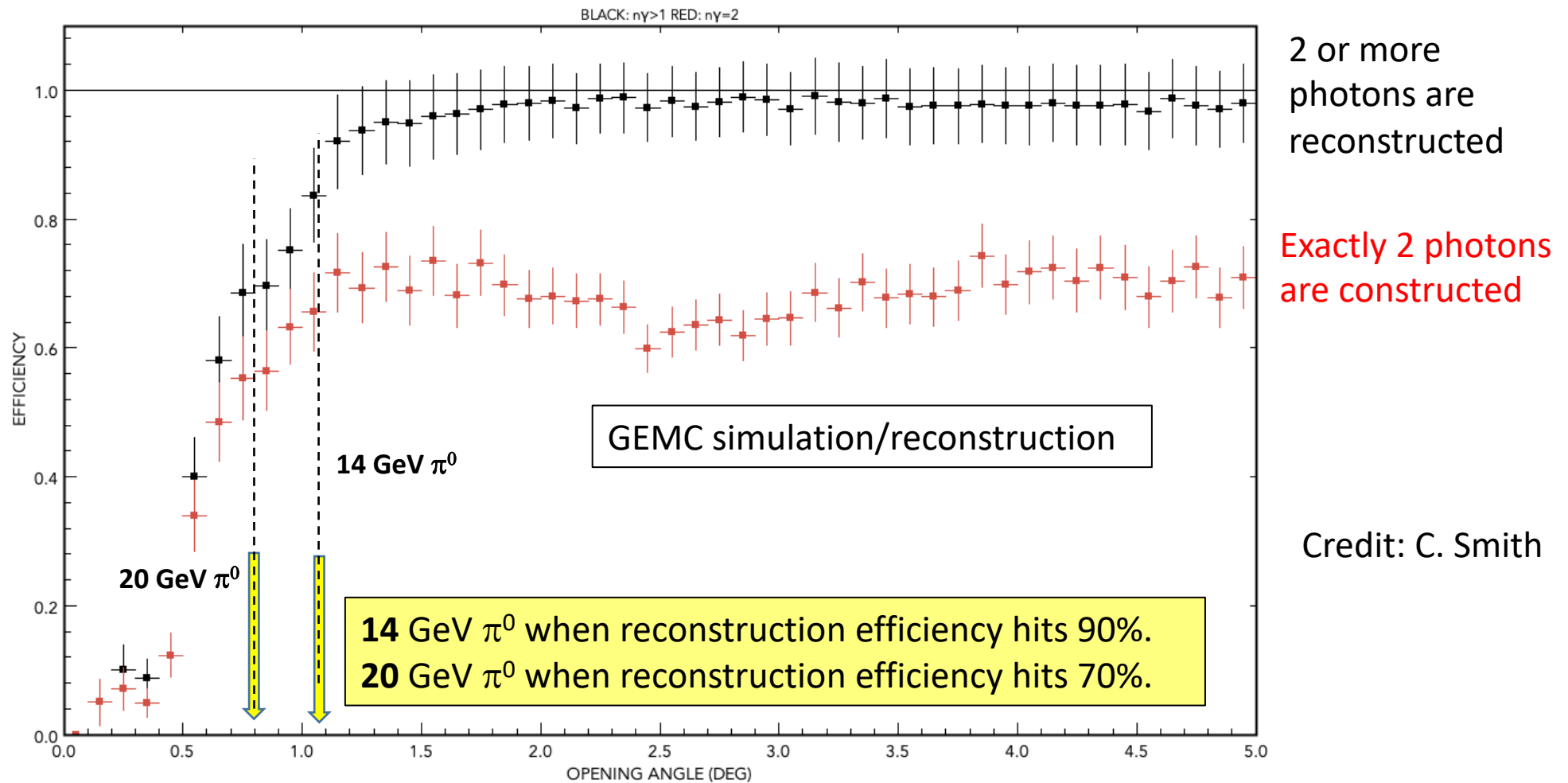
The proton identification in both the Forward Detector and in the Central Detector is sufficient.



π^0 and γ detection in ECAL at 24GeV

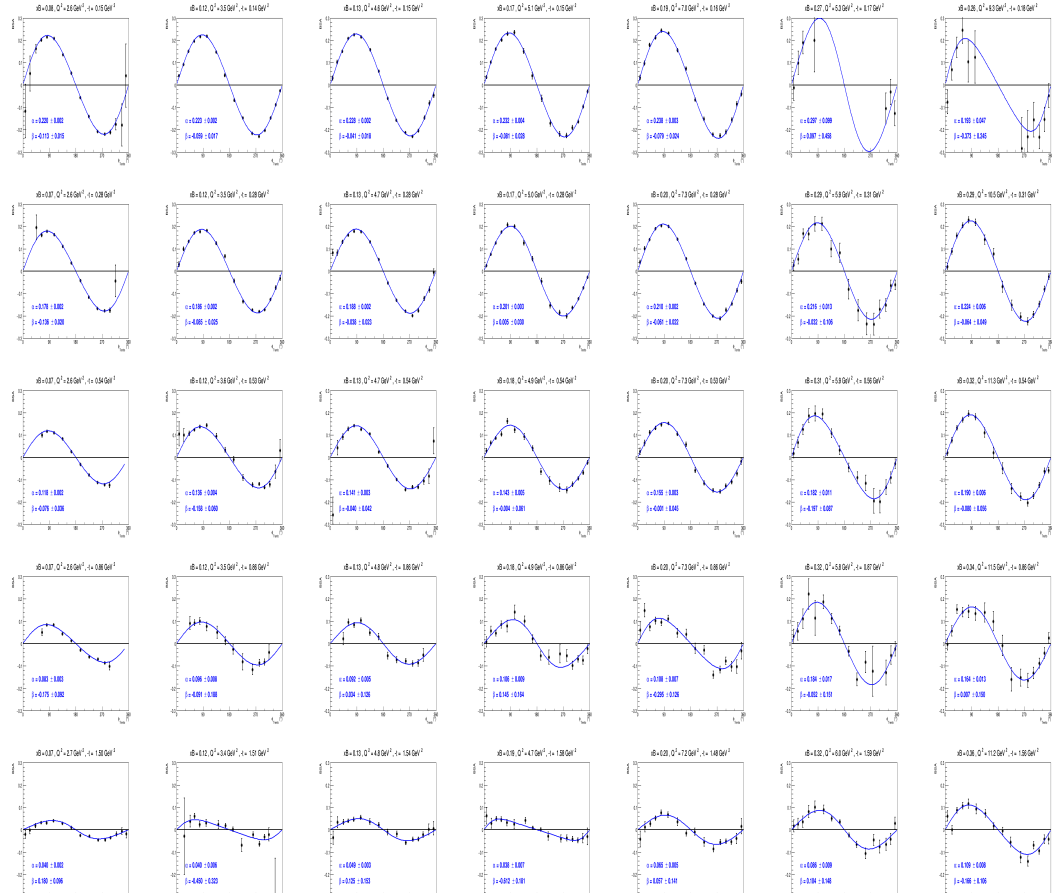
π^0 production is the largest background to DVCS.

- 1 γ escapes detection
- 2 γ merge to appear as 1 high energy γ .



- 60% of π^0 at 20 GeV are reconstructed in ECAL simulation.
- 70 – 85% of π^0 at 14 GeV are reconstructed in simulations.

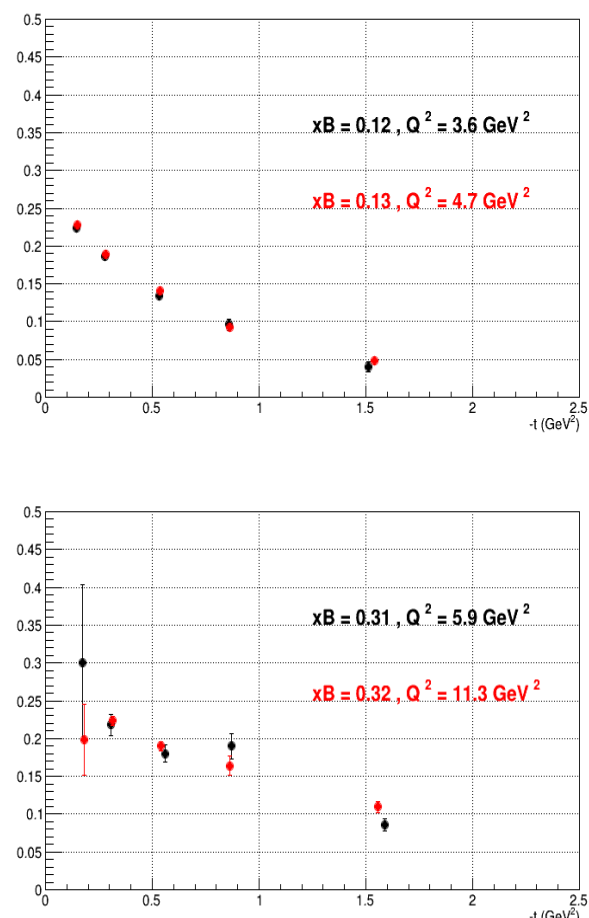
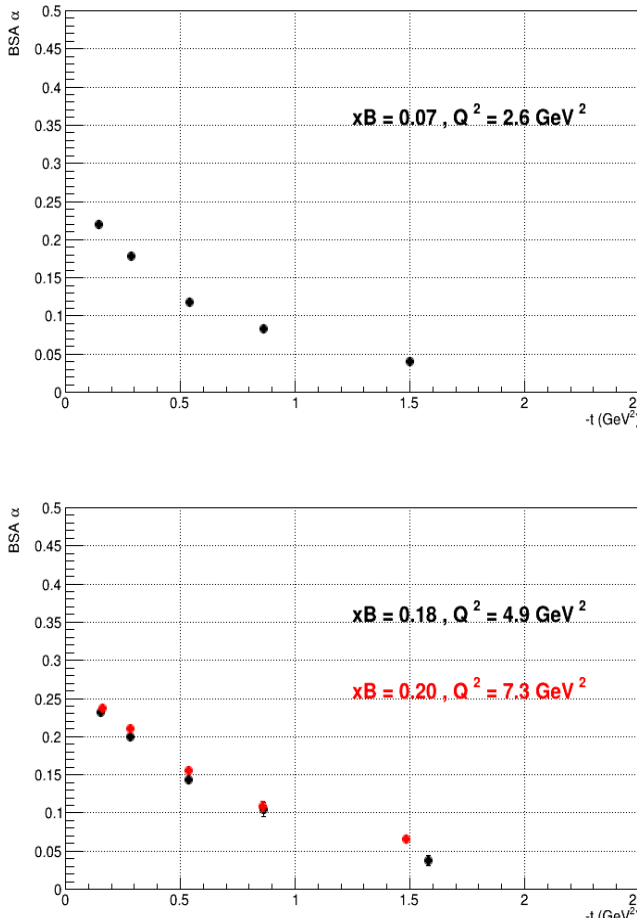
CLAS12 DVCS simulations/reconstruction at 22 GeV



Q^2

Credit: F.X. Girod

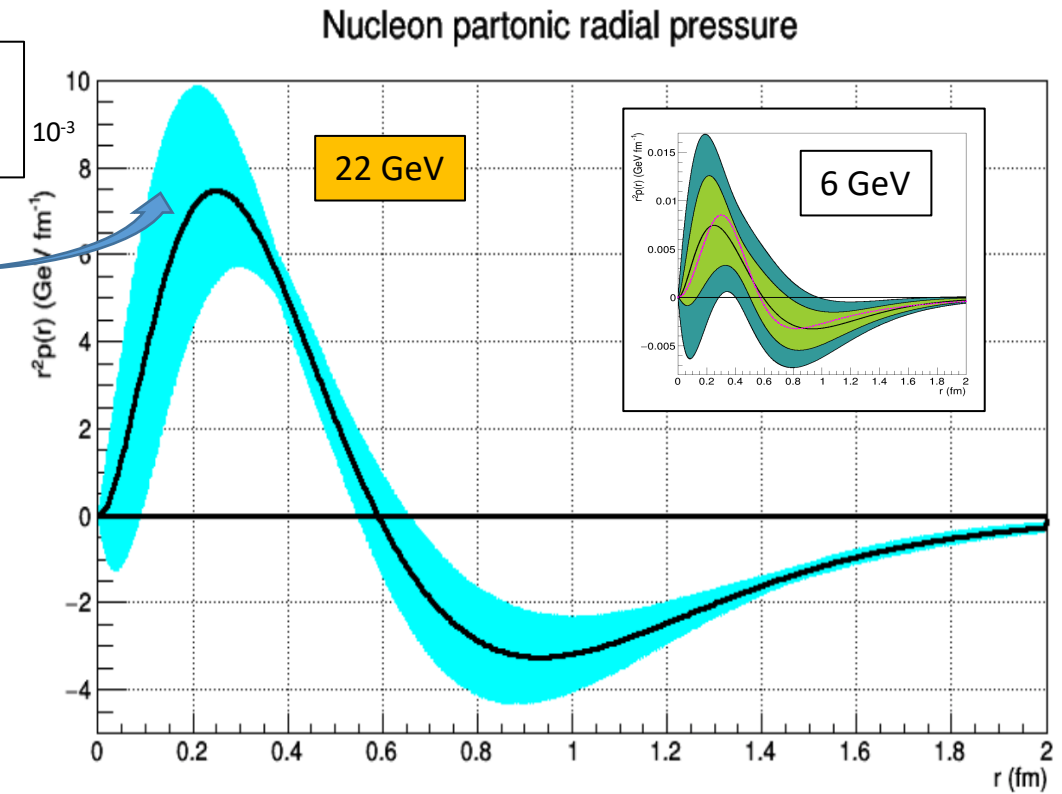
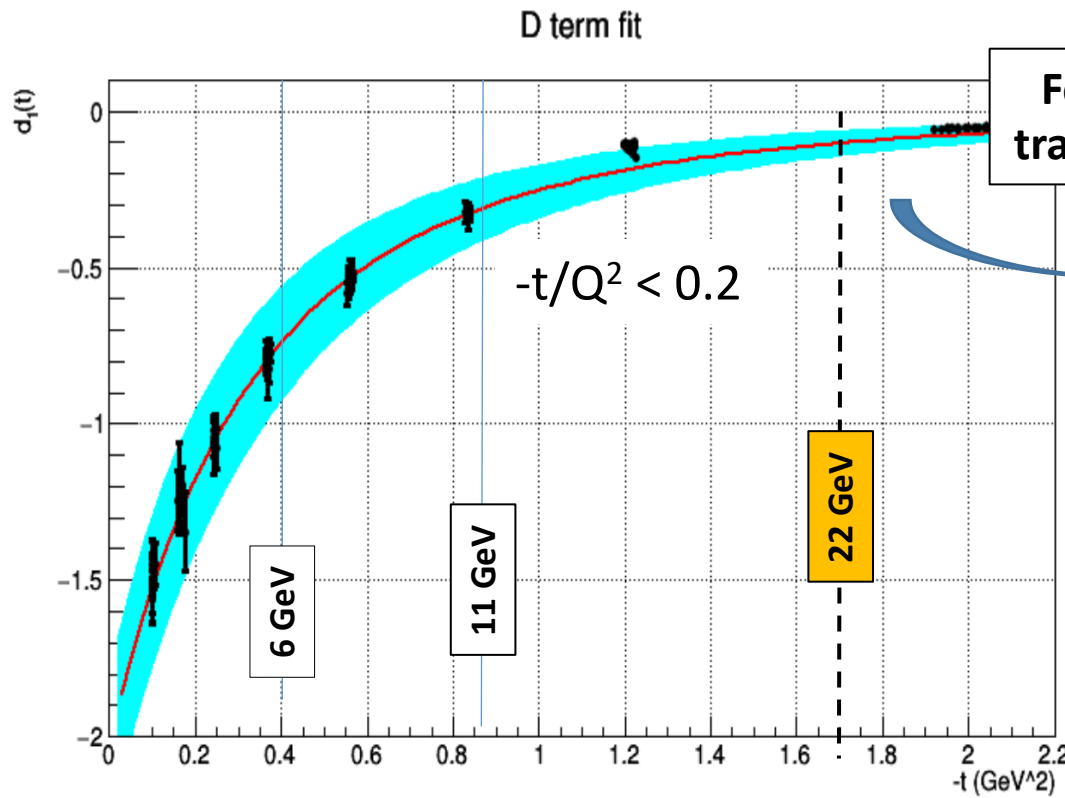
BSA – $\alpha \sin(\phi)$



The proton's D(t) and pressure at 22 GeV

Fitting the dispersion relation to $\text{Im} \mathcal{H}$, $\text{Re} \mathcal{H}$

$$-t/Q^2 < 0.2$$

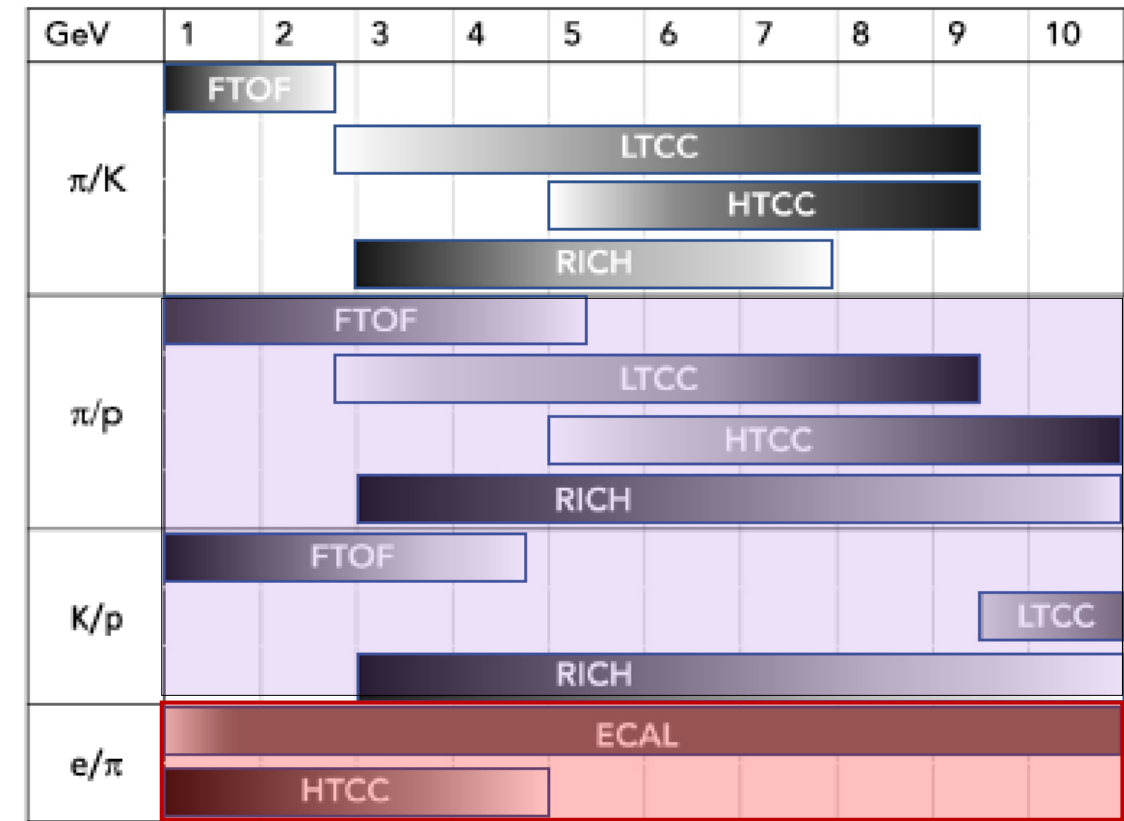
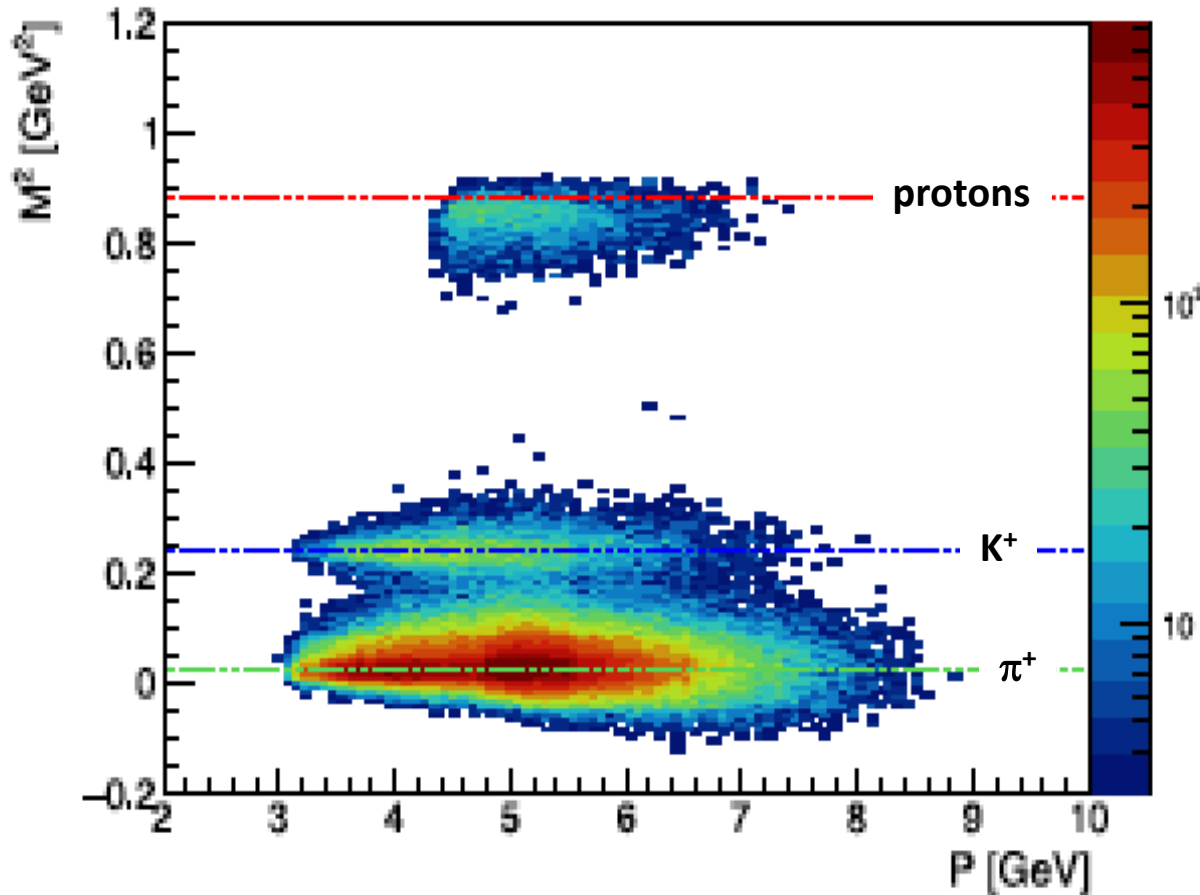


22 GeV will cover a large range in $-t$ and with reduced systematics uncertainties in the Fourier transform.

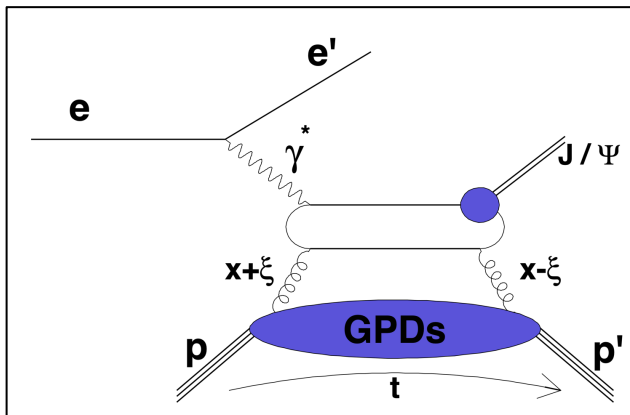
CLAS12 performance at 22 GeV - Summary

- CLAS12 tracking detector upgrade projects operation at luminosity $L \sim 2 \times 10^{35} \text{ cm}^{-2}\text{s}^{-1}$.
- Identification of the exclusive DVCS process.
- Large kinematic coverage in x_B , Q^2 , $-t$, for same CLAS12 setting.
- CLAS12 acceptances when operating long. polarized target remains as for unpolarized targets
- Transversely polarized target concept under development to access CFF \mathcal{E} and GFF $J(t)$ at large acceptance but at reduced luminosity (tbd).
- Detection of electrons at > 5 GeV relies on the 3-fold segmentation of the CLAS12 e.m. calorimeter combined with the exclusivity of the DVCS process.
- Measure TCS simultaneously with DVCS, provides direct access to CFFs $\text{Re}(\mathcal{H})$ and $\text{Im}(\mathcal{H})$ in BSA and FBA.

CLAS12 Charged particle ID in RICH



J/ ψ MC events reconstructed in CLAS12 at 24 GeV



Generated 20×10^6 J/ ψ events

